RSC Advances

ROYAL SOCIETY OF CHEMISTRY

www.rsc.org/advances

Graphene layers on Si-face and C-face surfaces and interaction with Si and C atoms in layer controlled graphene growth on SiC substrate

Xiaoye Shan, [a] *Qiang Wang,* *[a] *Xin Bian,* [a] *Wei-qi Li,* [b] *Guang-hui Chen,* [b] *and Hongjun Zhu** [a]

[a] Department of Applied Chemistry, College of Chemistry and Molecular Engineering, Nanjing Tech University, Nanjing 211816, P. R. China

[b] Department of Physics, Harbin Institute of Technology, Harbin 150001, P. R. China

[d] Department of Chemistry, Shantou University, Guangdong, Shantou,515063, P. R. China

*Corresponding E-mail: wangqiang@njtech.edu.cn, zhuhj@njtech.edu.cn.

Abstract

It is important to understand the interface and interaction between graphene layers and SiC surfaces as well as interaction of key intermediate Si and C atoms with these surfaces and interfaces in epitaxial graphene growth on SiC substrate. In this study, we used the DFT-D2 method, which includes the critical long-range van der Waals forces in graphene/SiC interaction, to study interface and interaction between mono-, bi-, and trilayer graphene and Si-face and C-face of SiC substrate as well as single Si and C atoms interaction with these surfaces and interfaces. Our results show that the interface including bottom layer of graphene and top layer of SiC occur a major reconstruction due to strong interaction of C-Si or C-C covalent bonds. The interaction energy of graphene bottom layer with C-face is significantly lower than that with Si-face, though there are stronger C-C covalent bonds and shorter interlayer distance at graphene/C-face than that at graphene/Si-face. In contrast, the interaction energy of second layer with bottom layer of graphene on C-face is obviously higher than that on Si-face. Especially, the top two layers almost float on bottom layer of trilayer graphene on Si-face. Furthermore, the bottom layer on Si-face with a metallic surface is of more chemical activity than that on C-face with a semiconducting surface. Compared with the interaction of Si and C atoms with these surfaces and interfaces, the results show that Si atom has a stronger interaction with both bare Si-face and C-face than C atom. Meanwhile, the interactions of Si and C atoms with bare Si-face are stronger than that with bare C-face. More importantly, once SiC surfaces are covered by first carbon layer, C atom prefers to stay on the interface

between existing carbon layer and Si-face or C-face rather than on the surface of existing carbon layer. In contrast, Si atom only prefers staying on the surface of existing carbon layer, not staying on the interface. The difference of Si and C atoms on this issue may result in an epitaxial growth of new carbon islands or layers at the interface between existing carbon layer and Si-face or C-face. All of these findings provide insight into the controlled growth of epitaxial graphene on SiC substrate and the design of graphere-SiC based electronic devices.

KEYWORDS: graphene, SiC, Si and C intermediates，interface and interaction, DFT-D2 calculation

Introduction

Epitaxial graphene growth on silicon carbide (SiC) substrate with high-quality and well-controlled thickness (or the number of layers) has been paid great interest and intensively researched since it not only can be compatible with current semiconductor technology (patterning *via* lithography) but also can offer a possibility of large-scale fabrication.[1-11] Many efforts have been devoted to achieving the epitaxial graphene growth by thermal decomposition of 4H- or 6H-SiC crystals in ultrahigh vacuum or under Ar atmospheric pressure conditions, in which Si atoms are sublimated preferentially and carbon atoms left behind would self-assemble into the graphene layers spontaneously.[11-24] Experimental studies have reported that graphene can be grown on both Si-terminated (0001) face (Si-face) and C-terminated $(000\bar{1})$ face (C-face) of the SiC substrate.[2, 3, 19, 23, 25-27] However, the growth features and consequent structures are significantly different for the graphene grown on Si-face and C-face surfaces. Si-face usually leads to growing a homogeneous graphene films with a controlled number of layers, whereas C-face tends to grow either multilayer graphene films with less homogeneous and rotational stacking or carbon nanotubes.[2, 3, 8, 28-36] In addition, for the Si-face, a complex buffer layer with $6\sqrt{3}\times 6\sqrt{3}R30^{\circ}$ periodic structure is thought to exist into interface between graphene layer and SiC surface, which strongly bonds with the Si-face, whereas the interfacial structure of graphene with the C-face is fairly different with that of the Si-face.[17, 37-43] Controversially, some studies have revealed that new graphene layers do grow from the interface between the buffer layer and SiC surface.[3, 21, 22, 39, 44-48] However, it has also been proposed that

new graphene layers would grow on the buffer layers, not directly on the SiC surface.[49] Furthermore, during the growth process of epitaxial graphene by thermal decomposition method, atomic Si and C are also the key intermediates interacting with the SiC surfaces and interface between existing graphene layer and SiC substrate. These issues strongly depend on the interface and interaction between graphene layers and SiC surfaces as well as interaction of Si and C atoms with these surfaces and interfaces. Thus, to achieve precisely controlled growth of high-quality graphene with specific layers, it is significantly important to obtain a more explicit understanding of the interfacial structures and interaction among Si/C atoms, graphene layers and SiC surfaces. Besides, it is also very useful for designing high performance graphene-SiC based electronic and optoelectronic devices.

The interfacial structures and interaction between graphene layers and SiC surface have been intensively studied by experimental and theoretical studies. Experimental results indicated that the first carbon layer is a graphene-like lattice, but without distinct graphene electronic properties.[14, 30, 37, 50, 51] Several recent studies showed that the distance is 2 Å from the first carbon layer to the Si-face.[27, 37] Nevertheless, A few other studies revealed that the first carbon layer is a corrugated layer, which 75% carbon atoms of the first carbon layer are at a distance of 2.4 Å and other 25% carbon atoms at 2.1 Å above the topmost Si layer.[52, 53] Meanwhile, several theoretical calculations also studied the interfacial structures of the graphene layers on SiC surface. They focused on the effect of the interfacial structures on its electronic properties. Furthermore, the common method used in these theoretical studies is the

local density approximation (LDA) or general gradient approximation (GGA) methods.[54, 55] However, it is well known that the LDA method overestimates the weakly bound van der Waals (vdW) interactions, while the GGA method underestimates such interactions.[56] In general, neither the LDA nor GGA methods would be reliable for understanding interface structures and interactions of graphene-SiC surfaces because they are known to poorly describe vdW forces.

In this work, we chose semi-empirical DFT-D2 Grimme's method, which including long-range vdW forces, to study the interfacial structure and interaction between graphene layers and SiC surfaces.[57, 58] On this basis, we further investigated key intermediates of Si and C atoms interaction with the bare Si-face, C-face, and the Si-face and C-face covered with the first carbon layer.

Computational methods

All the computations were performed with Vienna Ab initio simulation package (VASP) which based on density functional theory.[59, 60] The exchange-correlation interaction used the general gradient approximation (GGA) formulated by Perdew-Burke-Ernzerhof (PBE).[60] Long-range dispersion corrections have been taken into consideration within the DFT-D2 method.[61, 62] Electron interactions were described with projector augmented wave (PAW) pseudo potentials. The plane-wave basis set energy cutoff was restricted to 400 eV, and an 11×11×1 k-point mesh was used for the interaction of the Brillouin-zone. The electronic self-consistency criterion was set to 10^{-6} eV. Mulliken charge was calculated by DMol3 package.[63, 64]

The $\sqrt{3}\times\sqrt{3}R30^{\circ}$ periodic slab model was adopted in graphene-SiC systems,

which is known to be theoretically a good prototype for the experimental $6\sqrt{3}\times 6\sqrt{3}R30^\circ$ surface.[65] The unit cell was constructed using 6 silicon-carbon bilayers, monolayer, or bilayer, or trilayer graphene. These various graphene layers were placed on the Si-face or C-face in graphene-SiC systems, respectively, which includes at least 12 Å vacuum intervals to avoid interaction with their own images. To optimize the graphene-SiC systems, the graphene lattice constants were elastically adjusted to SiC lattice with 8% mismatch. While $2\sqrt{3}\times 2\sqrt{3}R30^\circ$ periodic slab model was adopted in adsorption systems of single Si/C atoms in order to avoid interaction with their own images. All graphene layers and the top four SiC bilayers were relaxed during optimization. Other two SiC bilayers in the bottom were fixed at their bulk lattice positions.

The interaction energy per unit cell between graphene layers is calculated by $\Delta E_g = (N\times E_{mono} - E_{bi/tri})/N$, where N is the number of graphene layers. There are 8 C atoms in each unit cell. E_{mono} and $E_{bi/tri}$ are the total energies of freestanding mono-, bi- or trilayer graphene per unit cell. The interaction energy per unit cell of graphene on SiC surfaces is calculated by $\Delta E_{g-SiC} = E_g + E_{SiC} - E_{g-SiC}$, where E_g, E_{SiC} and E_{g-SiC} are the total energy of freestanding graphene after elastic adjustment, SiC and graphene/SiC systems per unit cell, respectively.

Results and discussion

Fig. 1a shows optimized geometric structures of free mono-, bi-(AA and AB), trilayer (ABA and ABC) graphene with different stacking sequences. Each unit cell includes two C atoms in each graphene layer (as the blue dashed line in Fig. 1a). Fig.

1b shows optimized geometric structures of monolayer graphene adsorbed on Si-face and C-face. Each unit cell includes eight C atoms in each graphene layer (four graphene unit cells), and three C and three Si atoms in each SiC bilayer, respectively. The C-C bond length in freestanding graphene layer is 1.42 Å, while the C-C bond length is stretched to 1.54 Å in graphene-SiC systems (as listed in Table 1). The elastic stretching energy would amount to 0.69 eV/unit-cell.

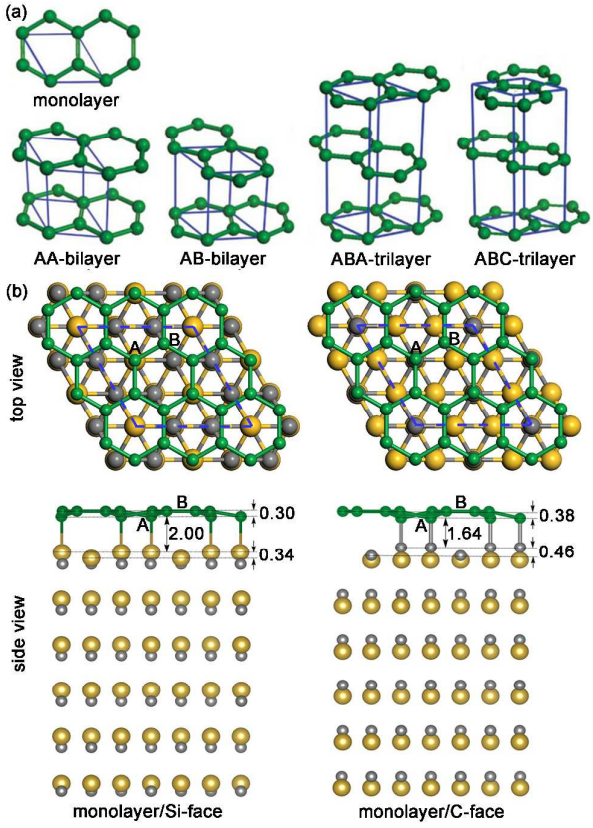

Fig. 1 (a) Optimized geometric structures of mono-, bi- (AA and AB) and trilayer (ABA and ABC) graphene. (b) The side and top views of monolayer graphene adsorbed on Si-face and C-face. Green, gray and yellow spheres represent graphene C atoms, C and Si atoms in SiC substrate, respectively. The unit cell is highlighted by blue solid or dashed line.

Table 1 Optimized geometric structure parameters of free mono-, bi- (AA and AB), trilayer (ABA and ABC) graphene, and these graphene layers adsorbed on Si-face and

C-faces. b is the C-C bond length in graphene. d_{12} and d_{23} are the interlayer distances between bottom and second layers, and second and third layers in graphene structures, respectively. $d_{g\text{-}SiC}$ are the distance from the bottom layer of graphene to Si-face or C-face. All values are given in angstrom (Å).

System \ Stacking		Monolayer	Bilayers		Trilayer	
			AB	AA	ABA	ABC
Graphene	b	1.42	1.42	1.42	1.42	1.42
	d_{23}	-	-	-	3.28	3.23
	d_{12}	-	3.24	3.49	3.28	3.24
G/Si-face	b	1.54	1.54	1.54	1.54	1.54
	d_{23}	-	-	-	3.35	3.36
	d_{12}	-	3.25/3.55	3.48/3.77	3.24/3.54	3.24/3.54
	$d_{g\text{-}SiC}$	2.00/2.64	2.00/2.62	2.00/2.61	2.00/2.62	2.00/2.62
G/C-face	b	1. 54	1.54	1.54	1.54	1.54
	d_{23}	-	-	-	3.40	3.35
	d_{12}	-	3.33/3.71	3.51/3.89	3.34/3.72	3.34/3.72
	$d_{g\text{-}SiC}$	1.64/2.48	1.64/2.47	1.64/2.47	1.64/2.47	1.64/2.48

The side view of Fig. 1b shows, for both Si-face and C-face, the graphene bottom layer and substrate top layer become significant distortion because there are strong covalent bonds at the interface. On Si-face, there are two lower C atoms at the diagonal of graphene hexagonal ring (labeled as the position A) bonding with two higher Si atoms on the Si-face surface by strong Si-C chemical bonds, such that the bond lengths is 2.00 Å. However, other higher C atoms of graphene hexagonal ring (labeled as the position B) have slightly longer separation distances (2.30 Å) to Si-face surface, and other one lower Si atom at the unit cell corners still remain an unsaturated dangling bonds. The adsorption energy of monolayer graphene on Si-face is 2.60 eV/unit-cell. Compared to the Si-face, it is noted that the distance from monolayer graphene to C-face is closer than that to Si-face. Two lower C atoms at

position A bond to two higher C atoms on the C-face surface by strong C-C covalent bonds, such that the bond length is only 1.64 Å. The graphene bonding atoms migrate downwards the substrate surface 0.38 Å, whereas the substrate surface bonding atoms move upwards the graphene 0.46 Å. The graphene/C-face layers have a major distortion as compared to the graphene/Si-face layers. Furthermore, it is well known the fact that the C-C bond is stronger than the Si-C bond. However, the adsorption energy of monolayer graphene on C-face is only 1.81 eV, significantly lower than that on the Si-face by 0.79 eV/unit-cell. Recent study[66] reported that the chemisorption energy between graphene and substrate is dominated by the interplay of bonding energy, Pauli repulsion and Van der Waals interactions, which differently depend on the graphene-substrate distance. Furthermore, the Pauli repulsion grows rapidly as the graphene-substrate distance decreases below 2.00 Å. In this case, the Pauli repulsion at a graphene/C-face distance of ~1.64 Å is stronger than that at a graphene/Si-face distance of ~2.00 Å. Relatively strong C-C bonding between graphene and C-face surface is counteracted partially by more strong Pauli repulsion of graphene-C-face. Thus, the adsorption energy of monolayer graphene on C-face is lower than that on the Si-face surface. This result indicates the adsorption energy of graphene layers on substrate surface decreases rapidly as the graphene-substrate distance decreases below 2.00 Å.

When bi- and trilayer graphene are adsorbed on Si-face and C-face, Table 1 shows that their interlayer distances from the bottom layer to substrate surface ($d_{g\text{-}SiC}$) are similar to that of the monolayer graphene on the Si-face and C-face. For the

Si-face, the interlayer distances from the bottom to second layer of graphene (d_{12}) are comparable to those of freestanding graphene structures. However, the interlayer distances from the second to third layer of graphene (d_{23}) are slightly longer than these of freestanding graphene structures by 0.07 Å for the ABA and 0.13 Å for the ABC stacking, respectively. As illustrated in Table 2, their interaction energies decrease with the increase of graphene layers: monolayer (2.60 eV/unit-cell) > bilayer (2.58 for AA and 2.56 for AB eV/ unit-cell) > trilayer (2.44 eV/unit-cell). However, similar to the graphene layers on Si-face, the interlayer distances of the d_{12} on the C-face are comparable to those of freestanding graphene structures. The interlayer distances of the d_{23} on the C-face are slightly longer than these of freestanding graphene structures 0.12 Å for the ABA and ABC, respectively. The interaction energies of graphene layers on C-face are obviously weaker than those on the Si-face. Their adsorption energies also decrease with the increase of graphene layers: monolayer (1.81 eV/unit-cell) > bilayer (1.74 for AA and 1.72 for AB eV/unit-cell) > trilayer (1.58 eV/unit-cell). Besides, the adsorption energies are not noteworthily different between AA and AB stacking, and between ABA and ABC stacking on the Si-face or C-face.

Table 2 The interaction energy of graphene layers with and without the SiC surfaces. $\Delta E_{g\text{-}SiC}$ is the interaction energy of the graphene layers on SiC surfaces. ΔE_g is the interaction energy between freestanding graphene layers. ΔE_{g12}, and ΔE_{g23} are the interaction energies between the bottom and second layers, the second and third layers in graphene/SiC systems, respectively. All values are given in eV/unite-cell.

System \ Stacking		Monolayer	Bilayers		Trilayer	
			AA	AB	ABA	ABC
Graphene	ΔE_g	-	0.22	0.30	0.62	0.62
	ΔE_{g23}	-	-	-	0.19,	0.19,
G/Si-face	ΔE_{g12}	-	0.15	0.20	0.09	0.09
	$\Delta E_{g\text{-}SiC}$	2.60	2.58	2.56	2.44	2.44
	ΔE_{g23}	-	-	-	0.20	0.20
G/C-face	ΔE_{g12}	-	0.21	0.27	0.17	0.17
	$\Delta E_{g\text{-}SiC}$	1.81	1.74	1.72	1.58	1.58

Next, we further compared the interaction energy between graphene layers with and without the SiC substrate. As listed in Table 2. The interaction energies between graphene layers on the SiC surface is significantly lower than that of freestanding graphene layers. For the bilayer graphene, the interaction energies follow the order ΔE_{g12}/Si-face (0.15 eV/unit-cell) < ΔE_{g12}/C-face (0.21 eV/unit-cell) ≈ ΔE_g (0.22 eV/unit-cell) for the AA stacking, and ΔE_{g12}/Si-face (0.20 eV/unit-cell) < ΔE_{g12}/C-face (0.27 eV/unit-cell) < ΔE_g (0.30 eV/unit-cell) for the AB stacking, respectively. In addition, the interaction energies of the AB stacking are higher than that of the AA stacking, which are 0.05, 0.06, and 0.08 eV/unit cell on the Si-face, C-face, and without substrate, respectively. These energy results suggest that the AB stacking is more stable than the AA stacking on both the SiC surfaces. For the trilayer graphene, the interaction energies follow the order ΔE_{g12}/Si-face (0.09 eV/unit-cell) < ΔE_{g12}/C-face (0.17 eV/unit-cell) < ΔE_g (0.31 eV/unit-cell) for both ABA and ABC stacking, and ΔE_{g23}/Si-face (0.19 eV/unit-cell) ≈ ΔE_{g23}/C-face (0.20 eV/unit-cell) < ΔE_g (0.31 eV/unit-cell) for both ABA and ABC stacking, respectively. More interestingly, the adsorption energy between the bottom and second layers would decrease rapidly (about 0.10 eV for both ABA and ABC on the Si- and C-face) duo to

the attraction of the third layer for second layer. Especially, the interaction energy between the bottom and second layers E_{g12} is only 0.09 eV/unit-cell, significantly lower than that between the second and third layers ΔE_{g23} by 0.19 eV/unit-cell for both ABA and ABC stacking in graphene/Si-face systems. The result suggests the top two graphene layer only floats on the bottom layer bonded on the Si-face, which would be favorable for the new graphene layer growth from the interface. It should be noted that, in the graphene-SiC systems, the lattice constants of all graphene layers were elastically adjusted to SiC lattice with 8% mismatch. Actually, because of the weak interaction between the bottom and second layers, it is possible that the lattice constants of the top layers in graphene-SiC systems is mostly identical to that of freestanding graphene. This mismatch of lattice structure between top layers and bottom layer would induce a substantial variation in the interaction energy. Thereby, we further compared the interaction energy of graphene layers at different lattice constants. The results show that the mismatch of lattice structure between top layers and bottom layer in our calculations is thought to have minor effects on our conclusions.

Charge transfer

Structural and interaction energy results in Table 1 and 2 show that the bottom layer of the graphene structures could form strong chemical bonds with the Si-face or C-face, while the bottom, second, and third graphene layers bond with each other by weak van der Waals force. This can be further validated by analyzing the charge density distribution at interfaces in graphene/Si-face and graphene/C-face systems. To

better illustrate the charge distribution at interfaces, the charge density difference of mono- and bilayer graphene on Si-face and C-face are plotted on Fig. 2. The charge density difference refers to the variance between the total charge density of graphene/Si-face or graphene/C-face systems and the sum of the charge density of the separated graphene structures and SiC substrate with Si-face or C-face. The geometric structures of separated graphene structures and Si-face or C-face were kept the same as these in grapheme/Si-face and grapheme/C-face systems. The green regions in Fig. 2 represent the accumulation of electronic charges, while the red regions indicate the depletion of electronic charges.

Fig. 2a shows that there are major charge transfer and electronic polarization between the monolayer graphene and Si-face surface. The side view in Fig. 2a further confirms there are strong polar C-Si covalent bonds between monolayer graphene and Si-face. The Si atoms directly donate electrons to the C atoms at the position A. The top view in Fig. 2a shows that on the monolayer graphene, the electrons are localized significantly at C atoms at position A. Mulliken charge analysis further shows that the C atoms at position A accumulate - 0.43 e, while those at position B only deplete around + 0.06 e. Correspondingly, the Si atoms direct bonding C atoms at position A deplete +1.20 e, while other neighboring Si atoms only deplete about + 0.97 e. Next, for the bilayer graphene shown in Fig. 2c, there is neither significant charge accumulation nor depletion on the top layer of bilayer graphene on the Si-face. The bottom layer of bilayer graphene shows similar charge transfer and electronic polarization as that of the monolayer graphene shown in Fig. 2a.

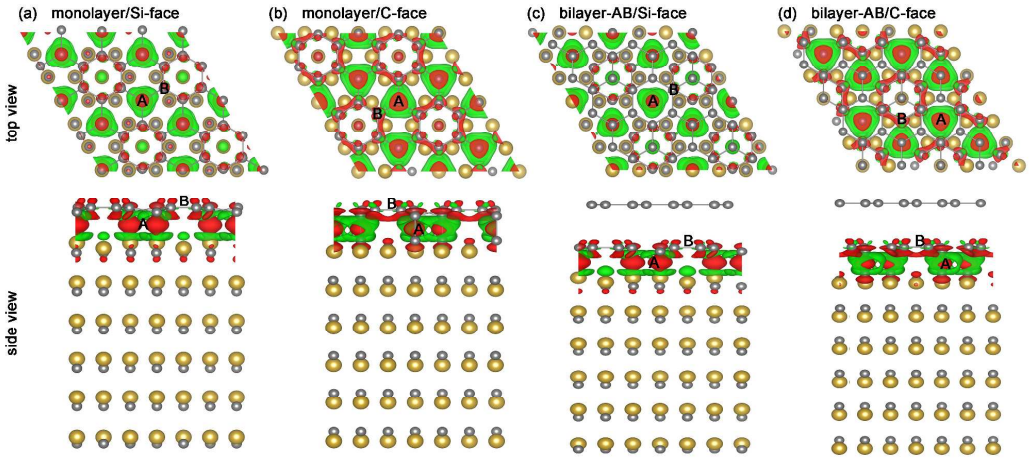

Fig. 2 Charge density difference plots of mono- and bilayer graphene absorbed on Si-face and C-face. The positive and negative charges are shown in red and green on charge density isosurface, respectively.

Compared to monolayer graphene on Si-face, there are also major electronic polarizations on the monolayer graphene in graphene/C-face system. However, charge transfer almost all comes from the neighboring graphene C atoms, while there are minor charge transfer between monolayer graphene and C-face. As illustrated Fig. 2b, C atoms at position B donate the electrons to the C atoms at position A from their σ-bands, and the C atoms in the C-face only share electrons with C atoms at position A partially. Mulliken charge analysis shows that on the monolayer graphene, the C atoms at position A only have - 0.11 e, while those at position B deplete around + 0.05 e. Correspondingly, in the C-face surface, the C atoms direct bonding C atoms at position A accumulate - 0.98 e, while other neighboring C atoms also accumulate about -0.96 e. Next, for the bilayer graphene shown in Fig. 2d, the bottom layer shows similar electronic polarization and charge transfer as that of the monolayer graphene

shown in Fig2b. The top layer of bilayer graphene has neither charge accumulation nor depletion as shown in Fig 2d.

Partial density of states

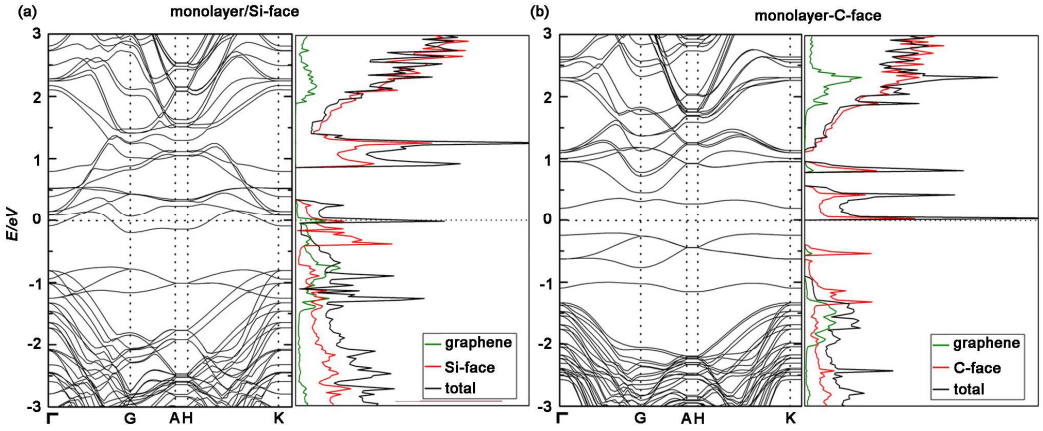

Fig. 3 Band structure (left) and density of state (DOS) of monolayer graphene on the (a) Si-face and (b) C-face. The Fermi level is assigned at 0 eV.

The differences of the monolayer graphene on Si-face and C-face in charge transfer and electronic polarization may induce distinct chemical reactivity. To further understanding their difference of chemical reactivity, we calculated the band structure and DOS of monolayer graphene on the Si-face and C-face. As shown in Fig. 3a, on the monolayer graphene/Si-face, band structure and DOS analyses reveal that the gap states close to the Fermi energy originate from the monolayer graphene and Si-face, which cross the Fermi level and become partially filled, resulting in metallic states. In contrast, on the monolayer graphene/C-face, a direct gap of about 0.50 eV appears in the band structure, making interface semiconducting. The PDOS shows that the valence band maximum and the conduction band minimum are mainly contributed by the C-face substrate, while the monolayer graphene almost have no contribution. The results suggest that the metallic interface states of monolayer on Si-face would be

much more reactive than the semiconducting interface states of the monolayer on C-face. Our results are consistent with the experimental report that the Si-face was in a half-filled metallic state, whereas the C-face was semiconducting.[37]

Interaction of single Si and C atoms

Atomic Si and C are the critical intermediates interacting with the SiC surfaces and interface between existing graphene layer and SiC substrate during the growth of epitaxial graphene on SiC substrate. An explicit understanding of the Si and C atoms interaction with these surfaces and interfaces is essential for probing the growth mechanism of epitaxial graphene on SiC substrate. In above section, the results show that the graphene on Si-face and C-face have different charge transfer, bonding type, and chemical activity. To directly examine the difference of atomic Si and C interaction with these surfaces and interfaces, in this section, we further investigate single Si and C atoms interaction with the bare Si- and C-faces, and the interface between the Si-face or C-face and first carbon layer. The optimized structures and interaction energies of single Si and C atoms on these surfaces are depicted in Fig. 4 and 5. The interaction energies of a single C or Si atom on these surfaces were defined as $\Delta E_a = E_{C(Si)-SiC}/E_{C(Si)-g-SiC} - E_{g-SiC} - E_{C(Si)}$ ($E_{C(Si)-SiC}$, $E_{C(Si)-g-SiC}$, E_{g-SiC}, and $E_{C(Si)}$ are the total energies of a fully optimized C/SiC, or Si/SiC complex, a fully optimized C/g/SiC, or Si/g/SiC complex, a fully optimized g/SiC complex, and a single C or Si atom, respectively).

As illustrated in Fig 4a and 5a, for a single Si and C atom, there are two stable adsorption sites on bare Si-face including three-fold μ_3-hollow and four-fold

μ_4-hollow sites. The Si adsorption energies are 7.77 eV at the μ_3-hollow site and 8.15 eV at the μ_4-hollow site, respectively. The C adsorption energies are 7.34 eV at the μ_3-hollow site and 7.71 eV at the μ_4-hollow site, respectively. In the case of the bare C-face, Si atom has only a stable four-fold μ_4-hollow site with adsorption energy of 6.27 eV. However, C atom has three stable surface adsorption sites as illustrated in Fig 5b. The adsorption energies of C atom at bridge-up, three-fold μ_3-hollow, and six-fold μ_6-hollow sites are 5.83, 5.98, and 6.71 eV, respectively. Compared with the interaction of single Si and C atoms on bare Si-face and C-face, the result of the adsorption energies show two trends: (1) single Si atom has a stronger interaction with both Si-face and C-face than C atom. (2) The interactions of single Si and C atoms with bare Si-face are stronger than that with bare C-face.

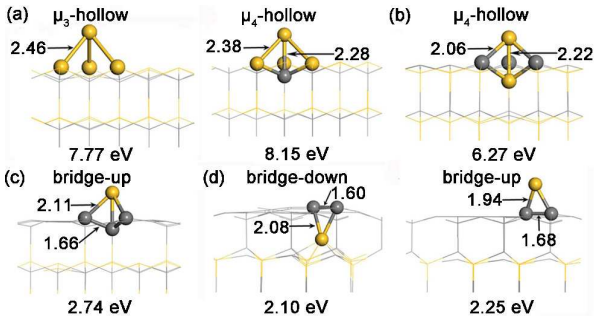

Fig. 4 Interaction of single Si atom with bare Si-face (a), C-face (b), and Si-face (c) and C-face (d) covered by the first carbon layer. Adjacent linking atoms are highlighted by the gray (C atom), and yellow (Si atom) balls, respectively. The bond lengths are shown in angstroms and interaction energies are shown in eV.

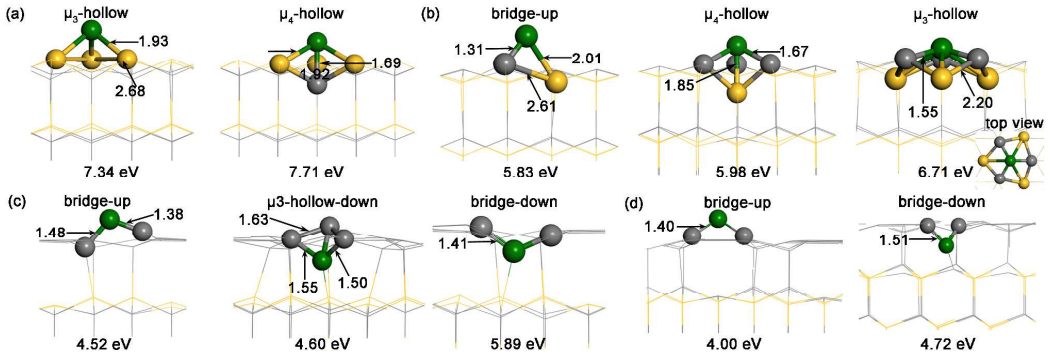

Fig. 5 Interaction of single C atom (green ball) with bare Si-face (a), C-face (b), and Si-face (c) and C-face (d) covered by the first carbon layer. Adjacent linking atoms are highlighted by the gray (C atoms of substrate), and yellow (Si atoms) balls, respectively. The bond lengths are shown in angstroms and interaction energies are shown in eV.

During the initial stage of the SiC thermal decomposition, with Si atoms continual sublimation, carbon atoms left behind would form covalent bonds among one another. Eventually, the first carbon layer would be formed on the Si-face or C-face. However, once Si-face or C-face is covered by the first carbon layer, it is necessary to answer the following questions: (1) are there significant differences in single Si and C atoms interaction with the covered Si-face and C-face by the first carbon layer? (2) Would Si and C atoms preferably stay on the interface between the exiting carbon layer and Si-face/C-face or adsorb on surface of exiting carbon layer?

As shown in Fig. 4c, for single Si atom on Si-face covered by the first carbon layer, there is only a stable surface site (bridge-up) on the first carbon layer with the interaction energy of 2.74 eV. However, we found that there is no any stable adsorption site at the interface between existing carbon layer and Si-face. In the case of C-face covered by the first carbon layer as shown in Fig. 4d, the C atom has only a stable surface adsorption site (bridge-up) with an adsorption energy of 2.25 eV and an

absorption site (bridge-down) with adsorption energy of 2.10 eV at the interface between existing carbon layer and C-face. Interestingly, these interaction energies are lower than that of Si atom on bare Si-face or C-face, but higher than that of Si atom adsorbed on freestanding monolayer graphene at 0.65 eV. This result suggests sublimated Si atoms would preferentially adsorb on Si-face or C-face before the first carbon layer formation, rather than on top of the growing carbon islands. These surface Si atoms would form the intermediate metastable Si-C bonds with the edge of the growing carbon islands. Thus, the surface Si atoms maybe play a role of stabilization and catalyst in growing carbon islands on the SiC surface. Furthermore, the interaction energies of Si atom on surface of existing carbon layer are higher than that of the interface interaction sites for the both Si-face and C-face. This result suggests, once SiC surfaces are covered by first carbon layer, Si atoms would prefer to stay on the surface of existing carbon layer, not stay at the interface between the existing carbon layer and Si-face or C-face.

For single C atom on Si-face covered by the first carbon layer, Fig. 5c shows that there are a stable surface site (bridge-up) on the first carbon layer with the interaction energy of 4.52 eV, and two subsurface sites (μ_3-hollow-down and bridge-down) under the first carbon layer with the interaction energies of 4.60 and 5.89 eV, respectively. In the case of C-face covered by the first carbon layer as shown in Fig. 5d, the C atom has only a stable surface adsorption site (bridge-up) with an adsorption energy of 4.00 eV and a subsurface absorption site (bridge-down) with adsorption energy of 4.72 eV. These adsorption energies are lower than that of C atom on bare Si-face or C-face, but

higher than that of C atom adsorbed on freestanding monolayer graphene at 1.86 eV. This result suggests, during the Si atoms sublimation stage, C atoms would preferentially adsorb on Si-face or C-face, rather than on top of the existing carbon layer. Thus, it is favorable to grow a flat carbon layer first than to grow into multilayer islands on the Si-face/C-face. In contrast to Si atom, the interaction energies of C atom at interface are higher than that of surface of the existing carbon layer for the both Si-face and C-face. This result suggests, once SiC surfaces are covered by first carbon layer, C atoms would prefer to stay on the interface between the existing carbon layer and Si-face or C-face, not on the surface of existing carbon layer. With the accumulation of C atoms, new carbon islands would be formed at the interface between existing carbon layer and Si-face or C-face, not on top of the existing carbon layer. It agrees with experimental findings that underneath of carbon layer on SiC substrate causes the accumulation of C atoms and a new carbon buffer layer was further formed at the interface between existing carbon layer and SiC substrate. [3, 21,67]

The intention of this work to find a general guideline for layer controlled graphene growth on SiC surbstrate, and also provide some understanding of the graphene-SiC interface for the potential electronic device design. Thus, this work focused on the interaction between graphene layers and Si- and C-face surfaces, and key inermediates of Si and C atoms interaction with the bare Si-face, C-face, and Si-face and C-face covered with one carbon layer. Our results from geometric structure, interaction energy, charge transfer, band structure and DOS further demonstrate that the buffer layer on Si-face with a metallic surface is distinctly

different with that on C-face with a semiconducting surface, which may induce different growth features and electronic properties. Furthermore, for bare Si-face and C-face, Si atom has a stronger interaction than C atom, and the interactions of Si and C atoms with Si-face are stronger than that with C-face. For the covered Si-face and C-face, C atom prefers to stay on the interface between buffer layer and Si-face or C-face, while Si atom only prefers staying on the surface of buffer layer. These results imply that new graphene layer would grow from the interface between the buffer layer and Si-face or C-face. Based on the findings from this work, we propose that, in order to achieve layer controlled growth, it is important to be able to tune the interaction among Si and C atoms, graphene layers, and SiC surfaces during different growth stages. This can be done through controlling the amount of the Si and C atoms decomposition, and modulating the buffer layer structure and buffer-layer-substrate separation during the thermal decomposition process of SiC, which could be controlled experimentally by the heating temperature, the heating rate, the vacuum pressure, and the composition of residual gas.

Conclusions

We used the DFT-D2 method to study the interface and interaction between the graphene layers and the Si-face and C-face of SiC substrate as well as key intermediate Si and C atoms interaction with these surfaces and interfaces. The results show that the interfacial structures of graphene bottom layer and SiC top layer have a large reconstruction due to the strong interaction of covalent bond. The interaction energies strongly depend on the interfacial structures. The interaction energy of

graphene bottom layer with C-face is significantly lower than that with Si-face, though there are stronger C-C covalent bonds and shorter interlayer distance at graphene/C-face than that at graphene/Si-face. In contrast, the interaction energy of second layer with bottom layer of graphene on C-face is obviously higher than that on Si-face. Especially, the top two layers almost float on bottom layer of trilayer graphene on Si-face. Charge transfer, DOS and Band structure analyses show that the bottom layer on Si-face with a metallic surface is more chemically active than that on C-face with a semiconducting surface. Compared with the interaction of single Si and C atoms with these surfaces and interfaces, the results show that single Si atom has a stronger interaction with both bare Si-face and C-face than C atom. Meanwhile, the interactions of single Si and C atoms with bare Si-face are stronger than those with bare C-face. More importantly, once SiC surfaces are covered by first carbon layer, C atom prefers to stay on the interface between existing carbon layer and Si-face or C-face rather than on the surface of existing carbon layer. In contrast, Si atom only prefers to stay on the surface of existing carbon layer, not stay on the interface. The results suggest new carbon islands or layers can be easily formed at the interface between SiC surface and existing carbon layer, not on top of existing carbon layer surface. The deeper insights into the interfacial structures and interaction among Si/C atoms, graphene layers and SiC surfaces from this study are expected to guide the layer controlled growth of graphene and the design of graphene-SiC based devices.

Acknowledgements

This work was supported by the National Natural Science Foundations of China

(21203094, 21373112, and 11104048), Natural Science Foundation of Guangdong Province (S2013010014476).

References

1. H. Hibino, H. Kageshima, M. Kotsugi, F. Maeda, F. Z. Guo and Y. Watanabe, *Physical Review B*, 2009, **79**.
2. W. Norimatsu, J. Takada and M. Kusunoki, *Physical Review B*, 2011, **84**.
3. W. Norimatsu and M. Kusunoki, *Physica E-Low-Dimensional Systems & Nanostructures*, 2010, **42**, 691-694.
4. K. Kimura, K. Shoji, Y. Yamamoto, W. Norimatsu and M. Kusunoki, *Physical Review B*, 2013, **87**.
5. M. Nagase, H. Hibino, H. Kageshima and H. Yamaguchi, *Nanotechnology*, 2008, **19**.
6. H. Hibino, H. Kageshima, F. Maeda, M. Nagase, Y. Kobayashi and H. Yamaguchi, *Physical Review B*, 2008, **77**.
7. W. Norimatsu and M. Kusunoki, *Physical Review B*, 2010, **81**.
8. W. Norimatsu and M. Kusunoki, *Chemical Physics Letters*, 2009, **468**, 52-56.
9. W. Norimatsu and M. Kusunoki, *Journal of Nanoscience and Nanotechnology*, 2010, **10**, 3884-3889.
10. H. Hibino, H. Kageshima, F. Z. Guo, F. Maeda, M. Kotsugi and Y. Watanabe, *Applied Surface Science*, 2008, **254**, 7596-7599.
11. C. Berger, Z. Song, X. Li, X. Wu, N. Brown, C. Naud, D. Mayou, T. Li, J. Hass, A. N. Marchenkov, E. H. Conrad, P. N. First and W. A. de Heer, *Science*, 2006, **312**, 1191-1196.
12. M. Morita, W. Norimatsu, H.-J. Qian, S. Irle and M. Kusunoki, *Applied Physics Letters*, 2013, **103**.
13. N. Ferralis, R. Maboudian and C. Carraro, *Physical Review Letters*, 2008, **101**.
14. H. Tetlow, J. P. de Boer, I. J. Ford, D. D. Vvedensky, J. Coraux and L. Kantorovich, *Physics Reports-Review Section of Physics Letters*, 2014, **542**, 195-295.
15. T. W. Hu, X. T. Liu, F. Ma, D. Y. Ma, K. W. Xu and P. K. Chu, *Nanotechnology*, 2015, **26**, 105708-105708.
16. H. Kageshima, H. Hibino, H. Yamaguchi and M. Nagase, *Physical Review B*, 2013, **88**.
17. H. Kageshima, H. Hibino, M. Nagase and H. Yamaguchi, *Applied Physics Express*, 2009, **2**.
18. C. Berger, Z. M. Song, T. B. Li, X. B. Li, A. Y. Ogbazghi, R. Feng, Z. T. Dai, A. N. Marchenkov, E. H. Conrad, P. N. First and W. A. de Heer, *Journal of Physical Chemistry B*, 2004, **108**, 19912-19916.
19. H. Huang and A. T. S. Wee, *Journal of Materials Research*, 2014, **29**, 447-458.
20. L. O. Nyakiti, R. L. Myers-Ward, V. D. Wheeler, E. A. Imhoff, F. J. Bezares, H. Chun, J. D. Caldwell, A. L. Friedman, B. R. Matis, J. W. Baldwin, P. M. Campbell, J. C. Culbertson, C. R. Eddy, Jr., G. G. Jernigan and D. K. Gaskill, *Nano Letters*, 2012, **12**, 1749-1756.
21. H. Huang, W. Chen, S. Chen and A. T. S. Wee, *Acs Nano*, 2008, **2**, 2513-2518.
22. W. Lu, J. J. Boeckl and W. C. Mitchel, *Journal of Physics D-Applied Physics*, 2010, **43**.
23. L. I. Johansson and C. Virojanadara, *Journal of Materials Research*, 2014, **29**, 426-438.
24. Luxmi, N. Srivastava, G. He, R. M. Feenstra and P. J. Fisher, *Physical Review B*, 2010, **82**.
25. L. Li and I. S. T. Tsong, *Surface Science*, 1996, **351**, 141-148.

26. Z. Guo, R. Dong, P. S. Chakraborty, N. Lourenco, J. Palmer, Y. Hu, M. Ruan, J. Hankinson, J. Kunc, J. D. Cressler, C. Berger and W. A. de Heer, *Nano Letters*, 2013, **13**, 942-947.

27. J. Borysiuk, R. Bozek, K. Grodecki, A. Wysmolek, W. Strupinski, R. Stepniewski and J. M. Baranowski, *Journal of Applied Physics*, 2010, **108**.

28. N. Ray, S. Shallcross, S. Hensel and O. Pankratov, *Physical Review B*, 2012, **86**.

29. M. Kusunoki, T. Suzuki, T. Hirayama, N. Shibata and K. Kaneko, *Applied Physics Letters*, 2000, **77**, 531-533.

30. J. L. Tedesco, B. L. VanMil, R. L. Myers-Ward, J. M. McCrate, S. A. Kitt, P. M. Campbell, G. G. Jernigan, J. C. Culbertson, C. R. Eddy, Jr. and D. K. Gaskill, *Applied Physics Letters*, 2009, **95**.

31. J. Hass, J. E. Millan-Otoya, P. N. First and E. H. Conrad, *Physical Review B*, 2008, **78**.

32. Z. G. Cambaz, G. Yushin, S. Osswald, V. Mochalin and Y. Goyotsi, *Carbon*, 2008, **46**, 841-849.

33. I. Forbeaux, J. M. Themlin, A. Charrier, F. Thibaudau and J. M. Debever, *Applied Surface Science*, 2000, **162**, 406-412.

34. J. Hass, F. Varchon, J. E. Millan-Otoya, M. Sprinkle, N. Sharma, W. A. De Heer, C. Berger, P. N. First, L. Magaud and E. H. Conrad, *Physical Review Letters*, 2008, **100**.

35. B. Huang, H. J. Xiang and S.-H. Wei, *Physical Review B*, 2011, **83**.

36. I. Deretzis and A. La Magna, *Applied Physics Letters*, 2013, **102**.

37. A. Mattausch and O. Pankratov, *Physical Review Letters*, 2007, **99**.

38. F. Varchon, R. Feng, J. Hass, X. Li, B. N. Nguyen, C. Naud, P. Mallet, J. Y. Veuillen, C. Berger, E. H. Conrad and L. Magaud, *Physical Review Letters*, 2007, **99**.

39. K. V. Emtsev, F. Speck, T. Seyller, L. Ley and J. D. Riley, *Physical Review B*, 2008, **77**.

40. S. Kim, J. Ihm, H. J. Choi and Y.-W. Son, *Physical Review Letters*, 2008, **100**.

41. H. Kageshima, H. Hibino, H. Yamaguchi and M. Nagase, *Japanese Journal of Applied Physics*, 2011, **50**.

42. C. Riedl, C. Coletti and U. Starke, *Journal of Physics D-Applied Physics*, 2010, **43**.

43. H. Matsui, F. Matsui, N. Maejima, T. Matsushita, T. Okamoto, A. N. Hattori, Y. Sano, K. Yamauchi and H. Daimon, *Surface Science*, 2015, **632**, 98-102.

44. J. B. Hannon, M. Copel and R. M. Tromp, *Physical Review Letters*, 2011, **107**.

45. J. Jobst, D. Waldmann, F. Speck, R. Hirner, D. K. Maude, T. Seyller and H. B. Weber, *Physical Review B*, 2010, **81**.

46. W. Norimatsu and M. Kusunoki, *Semiconductor Science and Technology*, 2014, **29**.

47. W. Norimatsu and M. Kusunoki, *Journal of Physics D-Applied Physics*, 2014, **47**.

48. W. Norimatsu and M. Kusunoki, *Physical Chemistry Chemical Physics*, 2014, **16**, 3501-3511.

49. S. Kopylov, A. Tzalenchuk, S. Kubatkin and V. I. Fal'ko, *Applied Physics Letters*, 2010, **97**.

50. N. Ogasawara, W. Norimatsu, S. Irle and M. Kusunoki, *Chemical Physics Letters*, 2014, **595**, 266-271.

51. J. Ristein, S. Mammadov and T. Seyller, *Physical Review Letters*, 2012, **108**.

52. D. Wang, L. Liu, W. Chen, X. Chen, H. Huang, J. He, Y.-P. Feng, A. T. S. Wee and D. Z. Shen, *Nanoscale*, 2015, **7**, 4522-4528.

53. B. K. Agrawal and S. Agrawal, *Physica E-Low-Dimensional Systems & Nanostructures*, 2013, **50**, 102-107.

54. J. P. Perdew and A. Zunger, *Phys. Rev. B: Condens. Matter*, 1981, **23**, 5048.

55. J. P. Perdew, K. Burke and M. Ernzerhof, *Phys. Rev. Lett.*, 1996, **77**, 3865-3868.

56. M. Vanin, J. J. Mortensen, A. K. Kelkkanen, J. M. Garcia-Lastra, K. S. Thygesen and K. W.

Jacobsen, *Phys. Rev. B: Condens. Matter*, 2010, **81**, 081408.

57. T. Bucko, J. Hafner, S. Lebegue and J. G. Angyan, *J. Phys. Chem. A*, 2010, **114**, 11814-11824.

58. S. Grimme, *J. Comput. Chem.*, 2006, **27**, 1787-1799.

59. E. Sanville, S. D. Kenny, R. Smith and G. Henkelman, *Journal of Computational Chemistry*, 2007, **28**, 899-908.

60. X. Liu, L. Fu, N. Liu, T. Gao, Y. Zhang, L. Liao and Z. Liu, *Journal of Physical Chemistry C*, 2011, **115**, 11976-11982.

61. A. V. Rozhkov, G. Giavaras, Y. P. Bliokh, V. Freilikher and F. Nori, *Physics Reports-Review Section of Physics Letters*, 2011, **503**, 77-114.

62. Z. R. Robinson, P. Tyagi, T. M. Murray, C. A. Ventrice, Jr., S. Chen, A. Munson, C. W. Magnuson and R. S. Ruoff, *Journal of Vacuum Science & Technology A*, 2012, **30**.

63. B. Delley, *Journal of Chemical Physics*, 1990, **92**, 508-517.

64. B. Delley, *Journal of Chemical Physics*, 2000, **113**, 7756-7764.

65. K. V. Emtsev, F. Speck, T. Seyller, L. Ley and J. D. Riley, *Physical Review B*, 2008, **77**.

66. S. M. Kozlov, F. Vines and A. Goerling, *Journal of Physical Chemistry C*, 2012, **116**, 7360-7366.

67. Lauffer, P.; Emtsev, K. V.; Graupner, R.; Seyller, T.; Ley, L.; Reshanov, S. A.; Weber, H. B. *Physical Review B* **2008,** 77, (15).